

1 **Complete genome sequence and Benzophenone-3 mineralisation**  
2 **potential of *Rhodococcus* sp. USK10, a bacterium isolated from**  
3 **riverbank sediment.**

4 Joseph Donald Martin<sup>1</sup>, Urse Scheel Krüger<sup>2</sup>, Athanasios Zervas<sup>1</sup>, Morten Dencker  
5 Schostag<sup>2,3</sup>, Tue Kjærgaard Nielsen<sup>4</sup>, Jens Aamand<sup>2</sup>, Lars Hestbjerg Hansen<sup>4</sup>, Lea  
6 Ellegaard-Jensen<sup>1#</sup>

7

8 <sup>1</sup> Department of Environmental Science, Faculty of Technical Science, Aarhus University, Roskilde, Denmark

9 <sup>2</sup> Department of Geochemistry, Geological Survey of Denmark and Greenland (GEUS), Copenhagen K, Denmark

10 <sup>3</sup> Department of Biotechnology and Biomedicine, Technical University of Denmark, Kongens Lyngby, Denmark

11 <sup>4</sup> Department of Plant and Environmental Sciences, University of Copenhagen, Frederiksberg, Denmark

12

13 # Corresponding author: Lea Ellegaard-Jensen, [leael@envs.au.dk](mailto:leael@envs.au.dk)

14 **Abstract**

15

16 Benzophenone-3 (BP3) is an organic UV filter whose presence in the aquatic environment  
17 has been linked to detrimental developmental impacts in aquatic organisms such as coral  
18 and fish. The genus *Rhodococcus* has been extensively studied and is known for  
19 possessing large genomes housing genes for biodegradation of a wide range of  
20 compounds, including aromatic carbons. Here, we present the genome sequence of  
21 *Rhodococcus* sp. USK10, which was isolated from Chinese riverbank sediment and is  
22 capable of utilising BP3 as the sole carbon source, resulting in full BP3 mineralisation.  
23 The genome consisted of 9,870,030 bp in 3 replicons, a G+C content of 67.2%, and 9,722  
24 coding DNA sequences (CDSs). Annotation of the genome revealed that 179 of these  
25 CDSs are involved in metabolism of aromatic carbons. The complete genome of  
26 *Rhodococcus* sp. USK10 is the first complete, annotated genome sequence of a  
27 Benzophenone-3 degrading bacterium. Through radiolabelling, it is also the first  
28 bacterium proven to mineralise Benzophenone-3. Due to the widespread environmental  
29 prevalence of Benzophenone-3, coupled to its adverse impact on aquatic organisms, this  
30 characterisation provides an integral first step in better understanding the environmentally  
31 relevant degradation pathway of the commonly used UV filter. Given USK10's ability to  
32 completely mineralise Benzophenone-3, it could prove to be a suitable candidate for  
33 bioremediation application.

34

35 **Keywords:** Oxybenzone, UV filter, biodegradation, whole genome sequencing,  
36 *Rhodococcus*

37 **1. Introduction**

38

39 Benzophenone-3 (BP3; 2-hydroxy-4-methoxybenzophenone; Oxybenzone) is an organic  
40 UV filter typically used in personal care products to protect the skin from harmful solar  
41 radiation. Organic UV filters have an aromatic chemical structure that allows for the  
42 absorption and stabilisation of both UVA (315-400 nm) and UVB (280-315 nm) radiation  
43 [1]. BP3 has been implemented as an active ingredient in sunscreens, cosmetics, and  
44 plastic products for decades, and is still one of the most commonly used UV filters  
45 worldwide. BP3 has been detected in surface waters, sediments and organisms within  
46 various environments including remote areas such as seawater of the Polar Regions [2,3].

47 Elevated concentrations of BP3 in the aquatic environment have been reported to result  
48 in adverse effects in aquatic organisms, such as deterioration of coral reefs and impaired  
49 reproduction potential in fish [4–6,1]. These detrimental factors have caused the use of  
50 BP3 containing sunscreens to be banned on the coasts of several countries, including the  
51 United States (Hawaii, U.S. Virgin Islands), Mexico, and Palau [1,4,7]. The chemical  
52 characteristics of BP3, and many other organic UV filters, is a cause of concern due to  
53 their high lipophilicity allowing for them to easily bioaccumulate in aquatic organisms and  
54 even in the body fluids of humans [2,8]. In addition, BP3 may also act as an endocrine  
55 disruptor in humans, influencing birth weight and gestational age [9]. The presence of  
56 BP3 in the aquatic environment worldwide begs the question of its persistence and,  
57 therefore, it is important to further research the biodegradation potential of BP3 facilitated  
58 by microorganisms found in natural environments.

59 In this study, we isolated and characterized the genome of *Rhodococcus* sp. USK10, to  
60 provide additional evidence of the genetic background of this BP3 mineralising bacterium.  
61 Currently, only two other bacterial strains, *Methylophilus* sp. strain FP-6 [10] and  
62 *Sphingomonas wittichii* strain BP14P [11], have been reported capable of degrading BP3.  
63 The phylogenetic characterisation of these strains was however solely based on 16S  
64 rRNA gene sequences and their genetic make-up was not investigated. Furthermore,  
65 both strains were hypothesized to be able to mineralise BP3, without, however, confirming  
66 it experimentally.

67 Here, we present the first complete and annotated genome of a BP3 degrader found in  
68 nature, including a potential linear megaplasmid and a smaller circular plasmid. Strain  
69 USK10 shows increased number of genes involved in catalyzing aromatic compounds  
70 compared to related *Rhodococcus* strains, which may indicate that it is a specialist strain.  
71 In addition, we present experimental data that prove the biodegradation of BP3 by  
72 *Rhodococcus* sp. USK10, when incubated in liquid media without any other carbon  
73 source.

74

## 75 **2. Materials and Methods**

76

### 77 *2.1 Isolation of Rhodococcus sp. USK10*

78 Strain USK10 was isolated from enrichment cultures originating from a Chinese riverbank  
79 sediment (GPS coordinates 25.569611, 119.781000). The sediment is characterised as  
80 unpolluted, having no known prior exposure to BP3. In short, the sediment was  
81 implemented into a series of enrichment cultures using radiolabeled BP3 to assess

82 degradation potential followed by a series of streak plating using BP3 enriched agar  
83 plates as the sole carbon source. Single colonies were picked and further asses for BP3  
84 mineralisation potential and later characterised, one of which being USK10.

85

86 *2.2 BP3 Biodegradation experiment*

87 Precultures for the mineralisation experiment were grown on R2B media supplemented  
88 with 100ppm BP3. After incubation at 20°C in the dark on an orbital shaker (120rpm) for  
89 3 days, extracts were centrifuged (12,000g x 5 minutes), washed twice, and resuspended  
90 in Difco™ Bushnell-Hass Broth (BHB). The mineralisation experiment was conducted in  
91 triplicate with each microcosm containing 5 mL of BHB with BP3 as the sole carbon  
92 source. Each USK10 microcosm had approximately  $1.4 \times 10^8$  cells, while the abiotic control  
93 had no cells. The initial BP3 concentration of each microcosm was 10 mg L<sup>-1</sup>, including  
94 [<sup>14</sup>C(U)]-labeled BP3 (Moravek Biochemicals Inc.; Brea, California, USA)  
95 amounting to 7055 DPM. The flasks further contained a 2 mL glass tube with 1 mL 1M  
96 NaOH serving as a basetrap to capture the evolved <sup>14</sup>CO<sub>2</sub> during BP3 mineralisation. The  
97 microcosms were incubated in the dark at 20°C and sampled once a day for 10 days. At  
98 each sampling time point, the NaOH was removed, replaced, and transferred to a plastic  
99 scintillation vial containing 10 mL of OptPhase HiSafe 3 scintillation cocktail (PerkinElmer,  
100 Waltman, MA, USA). All vials were counted for 10min using a Tri-Carb 2810 TR liquid  
101 scintillation analyzer (PerkinElmer, Waltman, MA, USA).

102

103 *2.3 DNA Extraction and library preparation*

104 High Molecular Weight DNA was extracted from USK10 grown on R2B liquid media. Prior  
105 to DNA extraction, strain purity was confirmed via streak plating on agar plates containing  
106 BP3 at a concentration of 250 ppm. DNA extractions were conducted using the Genomic  
107 Mini AX Bacteria kit (A&A Biotechnology, Gdynia, Poland). After extraction, the DNA was  
108 cleaned and concentrated using the Genomic DNA Clean & Concentrator kit (Zymo  
109 Research, Irvine, CA, USA) to remove any impurities that may have been present in the  
110 extracts. Concentration and quality of the DNA extracts were measured using Qubit 2.0  
111 Fluorometer with the 1x DS DNA Assay (Invitrogen, Carlsbad, CA, USA) and NanoDrop  
112 Spectrophotometer ND-1000 (Thermo Fisher Scientific, Walther, MA, USA), respectively.  
113 For Illumina sequencing an Illumina Nextera XT library was prepared for paired-end  
114 sequencing on an Illumina NextSeq550 (Illumina Inc., San Diego, CA, USA) according to  
115 the manufacturer's protocol. For Oxford Nanopore sequencing, a library was prepared  
116 using the Rapid Sequencing kit (SQK-RBK004) according to the manufacturer's  
117 instructions. Sequencing was performed on a MinION (Oxford Nanopore Technologies,  
118 Oxford, UK) with a FLO-MIN106 flow cell, controlled using MinKnow (19.10.1).

119

#### 120 *2.4 Bioinformatics analyses*

121 Sequencing adapters for Illumina reads were trimmed with Trim Galore (0.6.4)  
122 (<https://github.com/FelixKrueger/TrimGalore>). Raw Nanopore fast5 reads were  
123 basecalled with GPU-Guppy (3.2.6+afc8e14). A long-read only assembly was created  
124 using Raven (1.2.2) [12] and subsequently polished with the Unicycler polish module from  
125 the Unicycler assembler (0.4.8) [13], which applies long-read polishing with Racon [14]  
126 and short-read polishing with Pilon [15]. The completeness of the genomes was verified

127 by mapping to reference using the Illumina and Nanopore reads with BBmap [16] and  
128 Minimap2 [17] under default settings, implemented in Geneious Prime v2020.2.4  
129 (Biomatters). Plasmid sequences were classified using MOB-suite (3.0.0) [18]. The  
130 assembled draft genome was annotated using Rapid Annotation using Subsystem  
131 Technology (RAST), an online prokaryotic genome annotation platform [19]. Genome  
132 completeness was evaluated using BUSCO v5.2.2 using the bacteria\_odb10 lineage and  
133 "genome" mode [20]. For 16S phylogenetic tree construction, 16S rRNA gene sequences  
134 of strains related to USK10 were retrieved by BLAST  
135 (<https://blast.ncbi.nlm.nih.gov/Blast.cgi>). The 16S rRNA gene sequences were collected  
136 and aligned with MAAFT [21] under default settings in Geneious Prime v2020.2.4. The  
137 alignment was subsequently used for the construction of a 16S rRNA based phylogenetic  
138 tree using RAxML [22] in Geneious Prime, specifically the Rapid Bootstrapping and  
139 search for best-scoring ML tree algorithm with 100 iterations. Whole genome-based  
140 phylogenetic analysis was conducted using the Genome Taxonomy Database (GTDB)  
141 [23,24]. The classify workflow (classify\_wf) of the Genome Taxonomy Database Toolkit  
142 (GTDB-Tk) was used to determined USK10's taxonomic assignment [25]. The workflow  
143 produced a list of genomes similar to that of USK10 along with ANI scores for comparison  
144 purposes. Those genome assemblies were retrieved via NCBI and implemented in the  
145 lineage workflow (lineage\_wf) of CheckM to assess the similarities of their core genomes  
146 [26]. The alignment produced via CheckM was uploaded to Geneious Prime. A  
147 phylogenetic tree was created using RAxML, which utilised the GTR GAMMA nucleotide  
148 model under the "Rapid Bootstrapping and search for besting-scoring ML tree" algorithm  
149 with 100 boostraps replicated.

150

151 **2.5 Data availability**

152 The genome and plasmid sequence of *Rhodococcus* sp. USK10 has been deposited in  
153 GenBank under the accession numbers CP076046-CP076048.

154

155 **3. Results and Discussion**

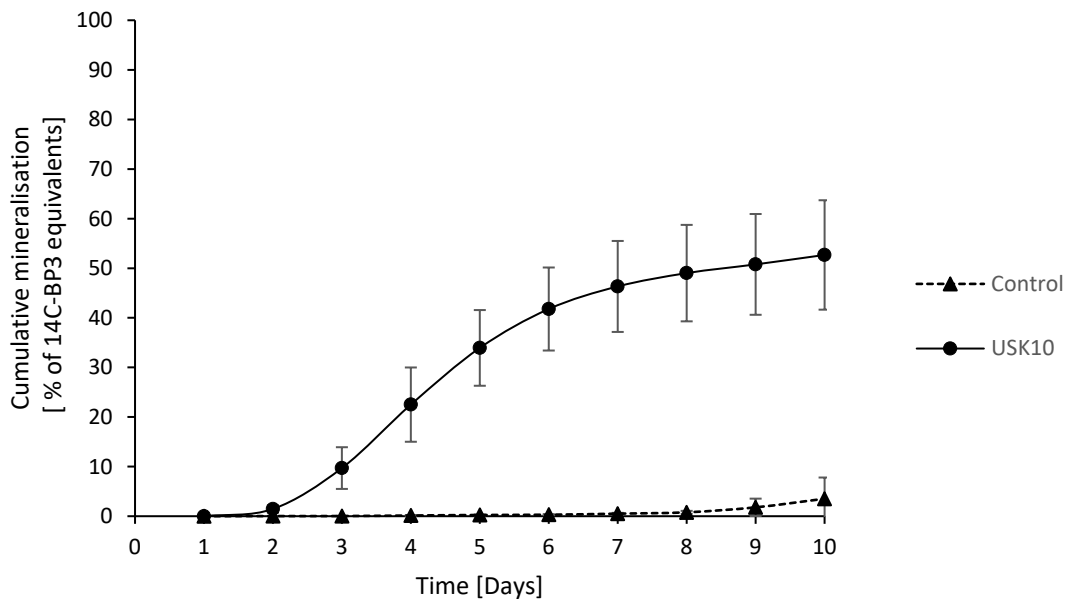
156

157 **3.1 BP3 degradation potential of *Rhodococcus* sp. USK10**

158 BP3 mineralization potential of *Rhodococcus* sp. USK10 was evaluated by measuring  
159 released carbon dioxide originating from labelled BP3 added as sole carbon source in a  
160 liquid medium microcosm. Figure 1 depicts the complete mineralisation of BP3 by strain  
161 USK10. USK10 starts to mineralise BP3 following a two days lag-phase. On the 10th day  
162 of the experiment, cumulatively 52.7% of the initial  $^{14}\text{C}$  label was collected in the form of  
163  $^{14}\text{CO}_2$  and complete mineralisation was assumed. The remaining labelled carbon fraction  
164 has likely been incorporated into construction of cellular biomass or metabolites [27].  
165 Comparatively, Lui and colleagues [28] studied biodegradation of BP3 in activated sludge  
166 microcosms, focusing on the biodegradation under various redox conditions. They  
167 reported that BP3 was completely biodegraded within 42 days of incubation. However,  
168 the half-lives of BP3 were observed to be relatively shorter at approximately 4-11 days.  
169 *Rhodococcus* sp. USK10 demonstrates the ability to mineralise BP3 within 10 days under  
170 aerobic conditions. Furthermore, degradation of BP3 has been shown in water via the  
171 UV/ $\text{H}_2\text{O}_2$  and UV/persulfate (UV/PS) reactions, but also using persulfate, metal ions,

172 PbO/TiO<sub>2</sub> and Sb<sub>2</sub>O<sub>3</sub>/TiO<sub>2</sub> and other chemicals [29–31]. However, these solutions are not  
173 considered “green solutions”.

174



175

176 **Figure 1.** Cumulative mineralisation of BP3 by strain USK10 in pure culture and an abiotic control over ten days. Mean  
177 values and standard deviation based on three replicates are shown for <sup>14</sup>CO<sub>2</sub> production relative to the initial amount  
178 of <sup>14</sup>C-BP3 added (<sup>14</sup>C<sub>0</sub>).

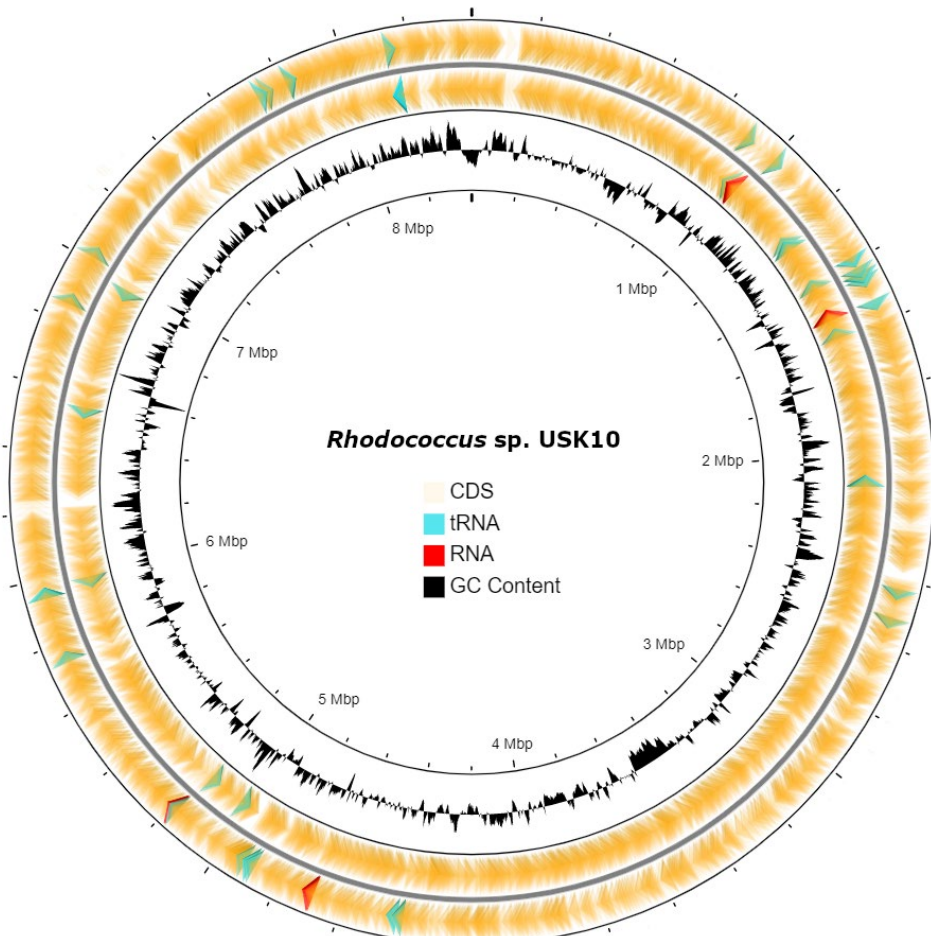
179

### 180 3.2 Genome analysis

181 The complete genome sequence of *Rhodococcus* sp. USK10 is composed of three  
182 replicons with a total assembly of 9,870,030 bp and a G+C content of 67.2%. The  
183 chromosome is 8,396,788bp (G+C content 67.6%), while the two mobilisable plasmids  
184 are 1,355,759 bp (linear, G+C content 64.6%) and 117,483 (circular, GC content 66%).  
185 The genomic map of the chromosome is presented in Figure 2. The circularity of the 3  
186 replicons was verified by mapping-to-reference runs using the Illumina and Nanopore

187 reads in Geneious Prime. For the chromosome and the small plasmid, these were  
188 successful. For the larger plasmid, manual forcing of circularity in Geneious Prime and  
189 subsequent mapping-to-reference yielded negative results for both the Illumina and  
190 Nanopore reads. *Rhodococcus* spp. as well as other Actinobacteria (e.g. *Micrococcus*  
191 spp. [32]) are known for having large linear plasmids housing genes coding for  
192 degradation potential [33,34]. The assembly is of high quality as revealed by BUSCO  
193 analysis (123 complete BUSCOs / 120 single copy and 3 double BUSCOs / 1 fragmented  
194 BUSCO / 99,2% coverage of bacteria\_odb10).

195



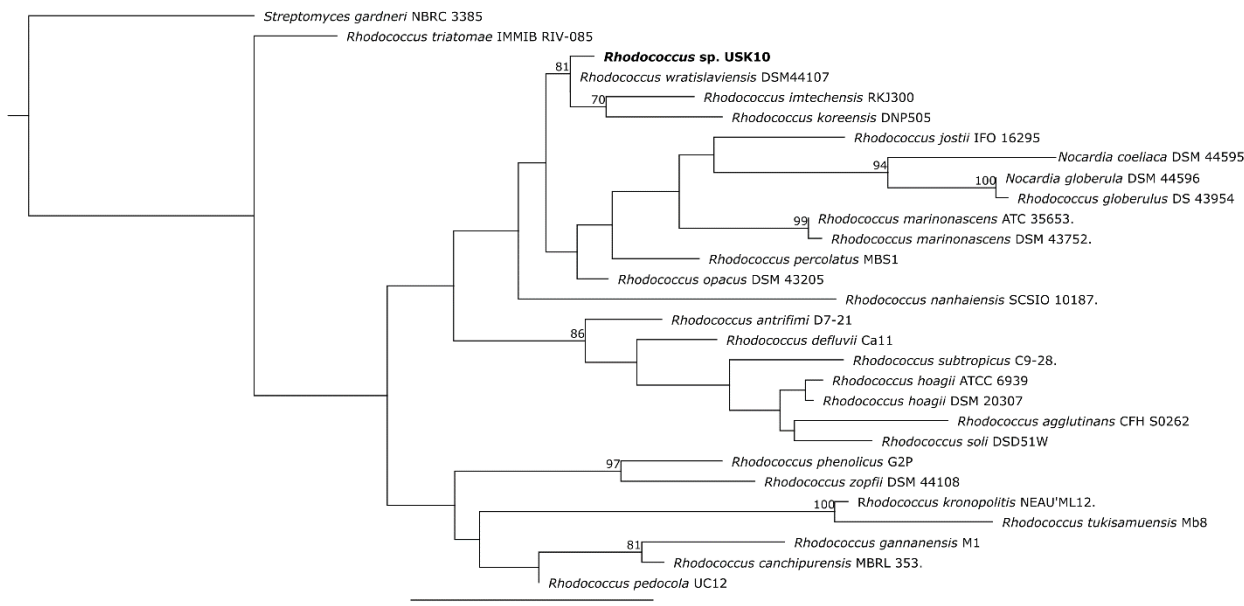
196

197 **Figure 1.** Circular map of *Rhodococcus* sp. USK10 chromosome. The two outer rings represent the coding sequences  
198 of the chromosome; the outermost being the forward strand and the innermost being the reverse strand. The inner  
199 most ring represents GC content. The G+C content of the chromosome is 67.2%. Created using CGview Server [35].

200

201 **3.3 Phylogenetic placement of *Rhodococcus* sp. USK10**

202 The phylogenetic analysis of both the 16S rRNA gene sequences and whole genome  
203 showed that USK10 is well supported within the *Rhodococcus* genus. Based on 16s rRNA  
204 gene sequences, *R. wratislaviensis* DSM 44107 and *R. koreensis* DNP505 are the closest  
205 relatives of USK10, having pairwise identities of 99.5% and 99.2%, respectively. Figure  
206 3 presents the phylogenetic tree based on 16S rRNA gene sequences.



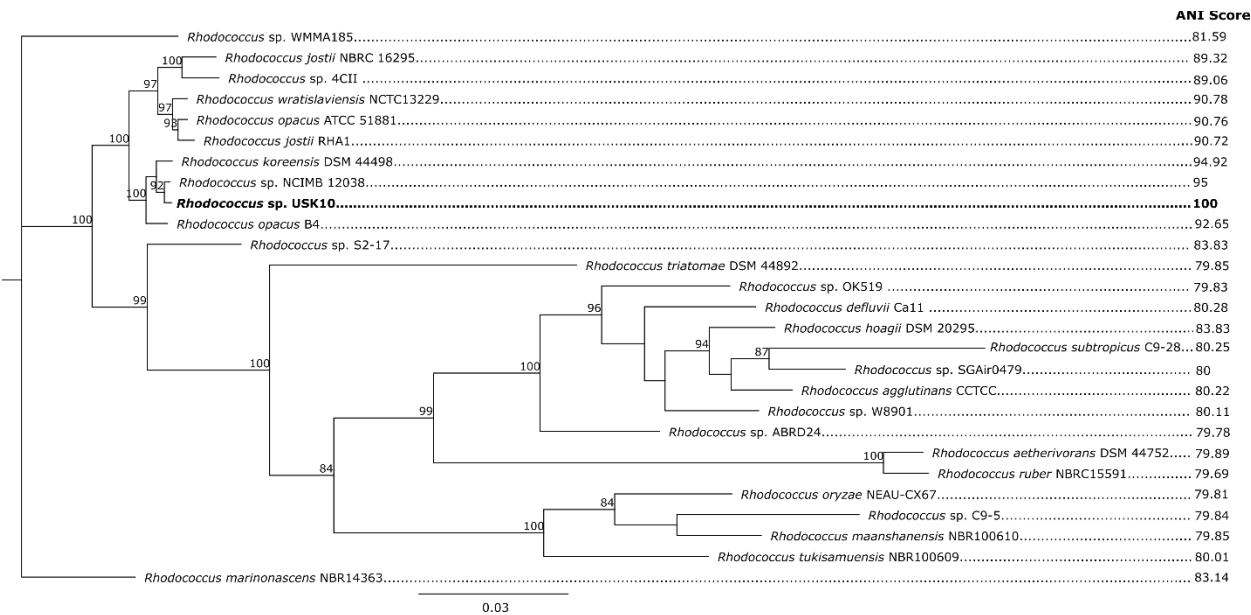
207

208 **Figure 3.** A phylogenetic tree based on 16S rRNA gene sequences showing the position of USK10 in relation to other  
209 *Rhodococcus* species and related genera of Actinobacteria. The nucleotide sequences were obtained from NCBI and  
210 aligned using the MAAFT alignment plugin via Geneious Prime 2020.2.4. The tree was constructed by RAxML (version  
211 8.2.11) in Geneious Prime 2020.2.4. Node numbers denote bootstrap support values above 60%. The nucleotide

212 module used was GTR GAMMA and the algorithm used was “Rapid Bootstrapping and search for the best-scoring ML  
213 tree” with 100 replicates. Bar, 0.02 substitutions per nucleotide position.

214

215 For whole genome analysis, GTDB-Tk classified the bacterial genomes based on  
216 phylogeny of 120 marker genes and ANI [25]. The ANI scores of each genome in relation  
217 to USK10 are presented jointly with the CheckM whole genome tree in Figure 4. From  
218 this analysis, the *Rhodococcus* strain determined to be the most related to USK10 was  
219 *Rhodococcus* sp. NCIMB 12038 with an ANI score of 95. This borders the species  
220 demarcation threshold. The next most related bacterium was *Rhodococcus koreensis*  
221 DSM 44489 which had an ANI score of 94.92. Considering the limited number of available  
222 *Rhodococcus* genomes, the exact ANI threshold for species affiliation is not certain. It  
223 has been seen on other bacterial groups (e.g. the *Bacillus cereus* group [36], the genus  
224 *Serratia* [37]), that this threshold ranges between 92 and 96%. Based on the topology of  
225 both the 16S rRNA sequences and the whole genome comparison, USK10 can be  
226 definitely placed and is well supported within the *Rhodococcus* genus. Additional  
227 characterisation analyses, such chemotaxonomic and biochemical assays, which are  
228 outside the scope of this study, would need to be conducted to assign proper taxonomic  
229 assessment to strain USK10 as well as strain NCIMB 12038 to be entirely confident.



230

231 **Figure 4.** Phylogenetic tree constructed around the position of USK10 based on whole genome sequences using  
232 CheckM alignment. The genome sequences were obtained via the NCBI assembly database. The tree was constructed  
233 by RAxML (version 8.2.11) in Geneious Prime 2.0. The nucleotide substitution model used was GTR GAMMA and the  
234 algorithm used was “Rapid Bootstrapping and search for the best-scoring ML tree” with 100 replicates. Node numbers  
235 denote bootstrap support values above 80%. Score values on the right indicate ANI scores obtained via whole genome  
236 comparison of USK10 using the GTDB-Tk classify workflow. The distance scale indicates 0.03 substitutions per  
237 nucleotide position.

238

### 239 3.4 Genome annotation

240 The annotated genome contains a total of 9,722 CDSs along with 61 RNA encoding  
241 genes. RAST was able to provide a general overview of the biological features within the  
242 genome, achieving a subsystem coverage of 39% of the annotated genes, 3,817  
243 subsystem feature counts. Of those counts, 179 were responsible for metabolism of  
244 aromatic compounds, some of which are likely involved in the degradation process of  
245 BP3. Out of the six enzyme classes, five are present in the coding sequences, which

246 involve the metabolism of aromatic compounds (26 hydrolases, 5 isomerases, 15 lyases,  
247 and 63 oxidoreductases.). Additionally, 13 transfer proteins involved in the degradation  
248 process were identified. The remainder of the CDSs annotated for involvement in  
249 metabolism of aromatic compounds, 2 were part of the Pca regulatory protein PcaR  
250 family and 39 part of the Transcriptional regulator IclR family. Both these protein families  
251 have been well documented to be involved in the degradation of aromatic carbons and  
252 present in other *Rhodococcus* species [38]. In *Sphingomonas wittichii* RW1 and DC-6,  
253 the first step in the degradation of aromatic compounds is performed by a dioxygenase  
254 gene located on a megaplasmid. USK10 bears 6 dioxygenase on its linear megaplasmid,  
255 1 on the small circular plasmid and 65 dioxygenase on its chromosome. Interestingly, the  
256 1 dioxygenase on the small plasmid (3-carboxyethylcatechol 2,3-dioxygenase) is placed  
257 next to a FAD-binding monooxygenase (PheA/TfdB family, similar to 2,4-dichlorophenol  
258 6-monooxygenase) which is involved in the degradation of another phenolic compound,  
259 2,4-dichlorophenol. As another alternative, hydroxylases have been suggested to be  
260 implemented in the first step of BP3 biodegradation. USK10 possesses 11 hydroxylases  
261 on its megaplasmid, 1 on its small plasmid, and 26 on its genome. The megaplasmid  
262 contains 65 oxidoreductases that may also play a role in USK10's biodegradation  
263 potential of BP3. Further exploitation of the *Rhodococcus* sp. USK10 genome, and that  
264 of other degraders, could lead to more confident identification of potential genes and  
265 processes involved in the biodegradation of BP3. Transcriptome sequencing and  
266 potentially proteomics analysis of BP3 degrading bacteria may also illuminate the  
267 involved genes and pathways in BP3 and other aromatic compounds degradation.

268 In this regard, *Rhodococcus* sp. USK10 has the potential to be used in large scale efforts  
269 to clean BP3-contaminated water sustainably. A key point to be investigated is the  
270 survivability and persistence of USK10 in mixed cultures. Other efforts to use microbes  
271 for biodegradation of xenobiotics have revealed a plethora of factors that may impact the  
272 effect of such approaches that need to be investigated and addressed accordingly [39].

273

274 **Acknowledgements**

275 This project was funded by Aarhus University Research Foundation starting grant (AUFF-  
276 E-2017-7-21) and Rural Water and Food Security (PI RURAL), the European Commission  
277 (Contract No. PI/2017/382/-112).

278

279 **Conflict of interest**

280 No conflict of interest declared.

281

282 **Author contributions**

283 Conceptualization: Joseph Donald Martin, Urse Scheel Krüger; Methodology: Joseph  
284 Donald Martin, Athanasios Zervas, Urse Scheel Krüger, Tue Kjærgaard Nielsen;  
285 Validation: Joseph Donald Martin, Urse Scheel Krüger; Resources: Jens Aamand, Lars  
286 Hestbjerg Hansen, Lea Ellegaard-Jensen; Writing: Joseph Donald Martin, Athanasios  
287 Zervas, Urse Scheel Krüger, Tue Kjærgaard Nielsen; Review and Editing: Joseph Donald  
288 Martin, Athanasios Zervas, Urse Scheel Krüger, Morten Dencker Schostag, Tue  
289 Kjærgaard Nielsen, Jens Aamand, Lars Hestbjerg Hansen, Lea Ellegaard-Jensen;

290 Supervision: Lea Ellegaard-Jensen, Morten Dencker Schostag, Jens Aamand, Lars  
291 Hestbjerg Hansen.

292

293 **References**

- 294 1. He, T.; Tsui, M.M.P.; Tan, C.J.; Ng, K.Y.; Guo, F.W.; Wang, L.H.; Chen, T.H.; Fan, T.Y.; Lam, P.K.S.; Murphy, M.B. Comparative Toxicities of Four Benzophenone Ultraviolet Filters to Two Life Stages of Two Coral Species. *Science of The Total Environment* **2019**, *651*, 2391–2399, doi:10.1016/j.scitotenv.2018.10.148.
- 295 2. Tsui, M.M.P.; Leung, H.W.; Wai, T.-C.; Yamashita, N.; Taniyasu, S.; Liu, W.; Lam, P.K.S.; Murphy, M.B. Occurrence, Distribution and Ecological Risk Assessment of Multiple Classes of UV Filters in Surface Waters from Different Countries. *Water Research* **2014**, *67*, 55–65, doi:10.1016/j.watres.2014.09.013.
- 296 3. Emnet, P.; Gaw, S.; Northcott, G.; Storey, B.; Graham, L. Personal Care Products and Steroid Hormones in the Antarctic Coastal Environment Associated with Two Antarctic Research Stations, McMurdo Station and Scott Base. *Environmental Research* **2015**, *136*, 331–342, doi:10.1016/j.envres.2014.10.019.
- 297 4. Downs, C.A.; Kramarsky-Winter, E.; Segal, R.; Fauth, J.; Knutson, S.; Bronstein, O.; Ciner, F.R.; Jeger, R.; Lichtenfeld, Y.; Woodley, C.M.; et al. Toxicopathological Effects of the Sunscreen UV Filter, Oxybenzone (Benzophenone-3), on Coral Planulae and Cultured Primary Cells and Its Environmental Contamination in Hawaii and the U.S. Virgin Islands. *Arch Environ Contam Toxicol* **2016**, *70*, 265–288, doi:10.1007/s00244-015-0227-7.
- 298 5. Balázs, A.; Krifaton, C.; Orosz, I.; Szoboszlay, S.; Kovács, R.; Csenki, Z.; Urbányi, B.; Kriszt, B. Hormonal Activity, Cytotoxicity and Developmental Toxicity of UV Filters. *Ecotoxicology and Environmental Safety* **2016**, *131*, 45–53, doi:10.1016/j.ecoenv.2016.04.037.
- 299 6. DiNardo, J.C.; Downs, C.A. Dermatological and Environmental Toxicological Impact of the Sunscreen Ingredient Oxybenzone/Benzophenone-3. *Journal of Cosmetic Dermatology* **2018**, *17*, 15–19, doi:10.1111/jocd.12449.
- 300 7. Fitt, W.K.; Hofmann, D.K. The Effects of the UV-Blocker Oxybenzone (Benzophenone-3) on Planulae Swimming and Metamorphosis of the Scyphozoans *Cassiopea Xamachana* and *Cassiopea Frondosa*. *Oceans* **2020**, *1*, 174–180, doi:10.3390/oceans1040013.
- 301 8. Kim, S.; Choi, K. Occurrences, Toxicities, and Ecological Risks of Benzophenone-3, a Common Component of Organic Sunscreen Products: A Mini-Review. *Environment International* **2014**, *70*, 143–157, doi:10.1016/j.envint.2014.05.015.
- 302 9. Ghazipura, M.; McGowan, R.; Arslan, A.; Hossain, T. Exposure to Benzophenone-3 and Reproductive Toxicity: A Systematic Review of Human and Animal Studies. *Reproductive Toxicology* **2017**, *73*, 175–183, doi:10.1016/j.reprotox.2017.08.015.
- 303 10. Jin, C.; Geng, Z.; Pang, X.; Zhang, Y.; Wang, G.; Ji, J.; Li, X.; Guan, C. Isolation and Characterization of a Novel Benzophenone-3-Degrading Bacterium *Methylophilus* Sp. Strain FP-6. *Ecotoxicology and Environmental Safety* **2019**, *186*, 109780, doi:10.1016/j.ecoenv.2019.109780.

333 11. Fagervold, S.K.; Rohée, C.; Rodrigues, A.M.S.; Stien, D.; Lebaron, P. Efficient  
334 Degradation of the Organic UV Filter Benzophenone-3 by *Sphingomonas Wittichii*  
335 Strain BP14P Isolated from WWTP Sludge. *Science of The Total Environment*  
336 **2021**, *758*, 143674, doi:10.1016/j.scitotenv.2020.143674.

337 12. Vaser, R.; Šikić, M. *Raven: A de Novo Genome Assembler for Long Reads*; 2021;  
338 p. 2020.08.07.242461;

339 13. Wick, R.R.; Judd, L.M.; Gorrie, C.L.; Holt, K.E. Unicycler: Resolving Bacterial  
340 Genome Assemblies from Short and Long Sequencing Reads. *PLOS*  
341 *Computational Biology* **2017**, *13*, e1005595, doi:10.1371/journal.pcbi.1005595.

342 14. Vaser, R.; Sović, I.; Nagarajan, N.; Šikić, M. Fast and Accurate de Novo Genome  
343 Assembly from Long Uncorrected Reads. *Genome Res.* **2017**, *27*, 737–746,  
344 doi:10.1101/gr.214270.116.

345 15. Walker, B.J.; Abeel, T.; Shea, T.; Priest, M.; Abouelliel, A.; Sakthikumar, S.;  
346 Cuomo, C.A.; Zeng, Q.; Wortman, J.; Young, S.K.; et al. Pilon: An Integrated Tool  
347 for Comprehensive Microbial Variant Detection and Genome Assembly  
348 Improvement. *PLOS ONE* **2014**, *9*, e112963, doi:10.1371/journal.pone.0112963.

349 16. Bushnell, B.; Rood, J.; Singer, E. BBMerge – Accurate Paired Shotgun Read  
350 Merging via Overlap. *PLOS ONE* **2017**, *12*, e0185056,  
351 doi:10.1371/journal.pone.0185056.

352 17. Li, H. Minimap2: Pairwise Alignment for Nucleotide Sequences. *Bioinformatics*  
353 **2018**, *34*, 3094–3100, doi:10.1093/bioinformatics/bty191.

354 18. Robertson, J.; Nash, J.H.E. MOB-Suite: Software Tools for Clustering,  
355 Reconstruction and Typing of Plasmids from Draft Assemblies. *Microb Genom*  
356 **2018**, *4*, e000206, doi:10.1099/mgen.0.000206.

357 19. Aziz, R.K.; Bartels, D.; Best, A.A.; DeJongh, M.; Disz, T.; Edwards, R.A.; Formsma,  
358 K.; Gerdes, S.; Glass, E.M.; Kubal, M.; et al. The RAST Server: Rapid Annotations  
359 Using Subsystems Technology. *BMC Genomics* **2008**, *9*, 75, doi:10.1186/1471-  
360 2164-9-75.

361 20. Simão, F.A.; Waterhouse, R.M.; Ioannidis, P.; Kriventseva, E.V.; Zdobnov, E.M.  
362 BUSCO: Assessing Genome Assembly and Annotation Completeness with Single-  
363 Copy Orthologs. *Bioinformatics* **2015**, *31*, 3210–3212,  
364 doi:10.1093/bioinformatics/btv351.

365 21. Katoh, K.; Standley, D.M. MAFFT Multiple Sequence Alignment Software Version  
366 7: Improvements in Performance and Usability. *Molecular Biology and Evolution*  
367 **2013**, *30*, 772–780, doi:10.1093/molbev/mst010.

368 22. Stamatakis, A. RAxML-VI-HPC: Maximum Likelihood-Based Phylogenetic  
369 Analyses with Thousands of Taxa and Mixed Models. *Bioinformatics* **2006**, *22*,  
370 2688–2690, doi:10.1093/bioinformatics/btl446.

371 23. Parks, D.H.; Chuvochina, M.; Waite, D.W.; Rinke, C.; Skarszewski, A.; Chaumeil,  
372 P.-A.; Hugenholtz, P. A Standardized Bacterial Taxonomy Based on Genome  
373 Phylogeny Substantially Revises the Tree of Life. *Nat Biotechnol* **2018**, *36*, 996–  
374 1004, doi:10.1038/nbt.4229.

375 24. Parks, D.H.; Chuvochina, M.; Chaumeil, P.-A.; Rinke, C.; Mussig, A.J.; Hugenholtz,  
376 P. A Complete Domain-to-Species Taxonomy for Bacteria and Archaea. *Nat*  
377 *Biotechnol* **2020**, *38*, 1079–1086, doi:10.1038/s41587-020-0501-8.

378 25. Chaumeil, P.-A.; Mussig, A.J.; Hugenholtz, P.; Parks, D.H. GTDB-Tk: A Toolkit to  
379 Classify Genomes with the Genome Taxonomy Database. *Bioinformatics* **2020**, *36*,  
380 1925–1927, doi:10.1093/bioinformatics/btz848.

381 26. Parks, D.H.; Imelfort, M.; Skennerton, C.T.; Hugenholtz, P.; Tyson, G.W. CheckM:  
382 Assessing the Quality of Microbial Genomes Recovered from Isolates, Single Cells,  
383 and Metagenomes. *Genome Res.* **2015**, *25*, 1043–1055,  
384 doi:10.1101/gr.186072.114.

385 27. Bouchez, M.; Blanchet, D.; Vandecasteele, J.-P. The Microbiological Fate of  
386 Polycyclic Aromatic Hydrocarbons: Carbon and Oxygen Balances for Bacterial  
387 Degradation of Model Compounds. *Appl Microbiol Biotechnol* **1996**, *45*, 556–561,  
388 doi:10.1007/BF00578471.

389 28. Liu, Y.-S.; Ying, G.-G.; Shareef, A.; Kookana, R.S. Biodegradation of the Ultraviolet  
390 Filter Benzophenone-3 under Different Redox Conditions. *Environmental  
391 Toxicology and Chemistry* **2012**, *31*, 289–295, doi:10.1002/etc.749.

392 29. Lee, Y.-M.; Lee, G.; Zoh, K.-D. Benzophenone-3 Degradation via UV/H<sub>2</sub>O<sub>2</sub> and  
393 UV/Persulfate Reactions. *Journal of Hazardous Materials* **2021**, *403*, 123591,  
394 doi:10.1016/j.jhazmat.2020.123591.

395 30. Pan, X.; Yan, L.; Qu, R.; Wang, Z. Degradation of the UV-Filter Benzophenone-3 in  
396 Aqueous Solution Using Persulfate Activated by Heat, Metal Ions and Light.  
397 *Chemosphere* **2018**, *196*, 95–104, doi:10.1016/j.chemosphere.2017.12.152.

398 31. Wang, Z.; Deb, A.; Srivastava, V.; Iftekhar, S.; Ambat, I.; Sillanpää, M. Investigation  
399 of Textural Properties and Photocatalytic Activity of PbO/TiO<sub>2</sub> and Sb<sub>2</sub>O<sub>3</sub>/TiO<sub>2</sub>  
400 towards the Photocatalytic Degradation Benzophenone-3 UV Filter. *Separation and  
401 Purification Technology* **2019**, *228*, 115763, doi:10.1016/j.seppur.2019.115763.

402 32. Dib, J.R.; Wagenknecht, M.; Hill, R.T.; Farías, M.E.; Meinhardt, F. First Report of  
403 Linear Megaplasmids in the Genus *Micrococcus*. *Plasmid* **2010**, *63*, 40–45,  
404 doi:10.1016/j.plasmid.2009.10.001.

405 33. König, C.; Eulberg, D.; Gröning, J.; Lakner, S.; Seibert, V.; Kaschabek, S.R.;  
406 Schrömann, M. A Linear Megaplasmid, P1CP, Carrying the Genes for  
407 Chlorocatechol Catabolism of *Rhodococcus Opacus* 1CP. *Microbiology* **2004**, *150*,  
408 3075–3087, doi:10.1099/mic.0.27217-0.

409 34. Görtler, V.; Seviour, R.J. Systematics of Members of the Genus *Rhodococcus*  
410 (Zopf 1891) Emend Goodfellow et al. 1998. In *Biology of Rhodococcus*; Alvarez,  
411 H.M., Ed.; Microbiology Monographs; Springer: Berlin, Heidelberg, 2010; pp. 1–28  
412 ISBN 978-3-642-12937-7.

413 35. Stothard, P.; Wishart, D.S. Circular Genome Visualization and Exploration Using  
414 CGView. *Bioinformatics* **2005**, *21*, 537–539, doi:10.1093/bioinformatics/bti054.

415 36. Zervas, A.; Aggerbeck, M.R.; Allaga, H.; Güzel, M.; Hendriks, M.; Jonuškienė, I.;  
416 Kedves, O.; Kupeli, A.; Lamovšek, J.; Mülner, P.; et al. Identification and  
417 Characterization of 33 *Bacillus Cereus* Sensu Lato Isolates from Agricultural Fields  
418 from Eleven Widely Distributed Countries by Whole Genome Sequencing.  
419 *Microorganisms* **2020**, *8*, 2028, doi:10.3390/microorganisms8122028.

420 37. *Serratia Inhibens* Sp. Nov., a New Antifungal Species Isolated from Potato  
421 (*Solanum Tuberosum*) | Microbiology Society Available online:  
422 <https://www.microbiologyresearch.org/content/journal/ijsem/10.1099/ijsem.0.004270?crawler=true> (accessed on 1 November 2021).

424 38. Tropel, D.; van der Meer, J.R. Bacterial Transcriptional Regulators for Degradation  
425 Pathways of Aromatic Compounds. *Microbiology and Molecular Biology Reviews*  
426 **2004**, *68*, 474–500, doi:10.1128/MMBR.68.3.474-500.2004.

427 39. Hylling, O.; Nikbakht Fini, M.; Ellegaard-Jensen, L.; Muff, J.; Madsen, H.T.;  
428 Aamand, J.; Hansen, L.H. A Novel Hybrid Concept for Implementation in Drinking  
429 Water Treatment Targets Micropollutant Removal by Combining Membrane  
430 Filtration with Biodegradation. *Science of The Total Environment* **2019**, *694*,  
431 133710, doi:10.1016/j.scitotenv.2019.133710.

432